Journal of Nuclear Materials 499 (2018) 496–503

Contents lists available at ScienceDirect

Journal of Nuclear Materials

journal homepage: www.elsevier.com/locate/jnucmat

A dual-phase microstructural approach to damage and fracture of Ti_3SiC_2/SiC joints

Ba Nghiep Nguyen*, Charles H. Henager Jr., Richard J. Kurtz

Pacific Northwest National Laboratory, P.O. Box 999, Richland, WA 99352, United States

ARTICLE INFO

Article history:
Received 7 September 2017
Received in revised form
20 November 2017
Accepted 30 November 2017
Available online 5 December 2017

Keywords:
SiC
Fusion materials
Joining
Swelling
Neutron irradiation
Thermal expansion
Damage modeling
Finite element

ABSTRACT

The microcracking mechanisms responsible for Ti_3SiC_2/SiC joint damage observed at the macroscopic scale after neutron irradiation experiments are investigated in detail. A dual-phase microstructural approach to damage and fracture of Ti_3SiC_2/SiC joints is developed that uses a finely discretized two-phase domain based on a digital image of an actual microstructure involving embedded Ti_3SiC_2 and SiC phases. The behaviors of SiC and Ti_3SiC_2 in the domain are described by the continuum damage mechanics (CDM) model reported in Nguyen et al., *J. Nucl. Mater.*, 2017, 495:504–515. This CDM model describes microcracking damage in brittle ceramics caused by thermomechanical loading and irradiation-induced swelling. The dual-phase microstructural model is applied to predict the microcracking mechanisms occurring in a typical Ti_3SiC_2/SiC joint subjected to heating to 800 °C followed by irradiation-induced swelling at this temperature and cooling to room temperature after the applied swelling has reached the maximum swelling levels observed in the experiments for SiC and Ti_3SiC_2. The model predicts minor damage of the joint after heating but significant microcracking in the SiC phase and along the boundaries between SiC and Ti_3SiC_2 as well as along the bonding joint during irradiation-induced swelling and cooling to room temperature. These predictions qualitatively agree with the limited experimental observations of joint damage at this irradiation temperature.

1. Introduction

Developing methods for joining silicon carbide (SiC) to itself or other materials is needed to enable application of SiC ceramics and composites in future fusion reactors or nuclear systems since it is difficult to fabricate an entire composite structure without some joined sections. The international fusion materials community has recently irradiated and tested several joint types and compositions including Ti_3SiC_2/SiC composite joints in the High Flux Isotope Reactor (HFIR) reactor at Oak Ridge National Laboratory (ORNL) [1]. As discussed in Ref. [1], joining SiC to itself or to other materials presents several critical issues that have not been resolved and two key issues central to this technology are identified in Ref. [1]. The first issue is radiation-induced cracking and microcracking observed in limited neutron irradiation experiments conducted on several joints, with cracking observed in the joints and in the joined SiC material itself. The second issue is the lack of a widely accepted standard test method for joining that can be successfully irradiated and tested to provide high-quality strength data.

In a recent paper [2], we pointed to a general lack of predictive modeling tools that can either assist in designing a ceramic joint to withstand irradiation, or provide guidance to develop a joining method for SiC and its composites. To address this issue, we developed a continuum damage mechanics (CDM) model and implemented it in the ABAQUS finite element (FE) code to predict cracking of the torsion hourglass (THG) specimen's joint [1] made of the Ti_3SiC_2/SiC composite produced using displacement reactions between SiC and TiC [3]: $3TiC + 2Si \rightarrow Ti_3SiC_2 + SiC$ (3C-SiC polytype). Our previous work [2] helps understand joint behavior in the THG macroscopic structure following thermomechanical and irradiation exposures. To study in detail the microcracking mechanisms responsible for joint damage and fracture observed at the macroscopic scale, we develop a dual-phase microstructural approach in this paper that involves an actual microstructural domain containing SiC embedded in a MAX phase matrix (Ti_3SiC_2). The behaviors of SiC and Ti_3SiC_2 are described by the same CDM model reported in Ref. [2], and the dual-phase microstructure

* Corresponding author. Pacific Northwest National Laboratory, PO Box 999, MSIN: J4-55, Richland, WA 99352, United States.
E-mail address: Ba.Nguyen@pnnl.gov (B.N. Nguyen).

https://doi.org/10.1016/j.jnucmat.2017.11.054
0022-3115/

subjected to thermal expansion and irradiation-induced swelling is analyzed using ABAQUS.

2. Theoretical background

This paper uses the Nguyen et al. damage model for brittle ceramics to describe the occurrence and evolution of microcracking damage in the constituent SiC and Ti_3SiC_2 phases that form the Ti_3SiC_2/SiC composite joint [2]. The constitutive relations accounting for the thermal expansion and irradiation-induced swelling effects are written as:

$$\sigma_{ij} = C_{ijkl}(T,D)\left(\varepsilon_{kl} - \varepsilon^{\text{th}}_{kl} - \varepsilon^{\text{s}}_{kl}\right) = C^{0}_{ijkl}(T)(1-D)\left(\varepsilon_{kl} - \varepsilon^{\text{th}}_{kl} - \varepsilon^{\text{s}}_{kl}\right) = C^{0}_{ijkl}(T)(1-D)\varepsilon^{\text{m}}_{kl} \tag{1}$$

where $C_{ijkl}(T,D)$ is the material elastic stiffness tensor that varies with temperature T and is affected by the microcracking damage phenomenologically described by the damage variable, D. A linear stiffness reduction law of $C_{ijkl}(T,D)$ with D is used in Eq. (1) where $C^{0}_{ijkl}(T)$ is the initial stiffness tensor without material damage. ε_{ij}, $\varepsilon^{\text{th}}_{ij}$, $\varepsilon^{\text{m}}_{ij}$ and $\varepsilon^{\text{s}}_{ij}$ are the total, thermal, mechanical, and swelling strains, respectively. $\varepsilon^{\text{th}}_{ij}$ is given by:

$$\varepsilon^{\text{th}}_{ij} = \alpha_{ij}(T)\Delta T \tag{2}$$

and $\alpha_{ij}(T)$ is the temperature-dependent tensor of thermal expansion coefficients, and $\varepsilon^{\text{s}}_{ij}$ is based on a model proposed in Ref. [4]:

$$\varepsilon^{\text{s}}_{ij} = \begin{cases} S_{ij}(T) & \text{if } i=j \text{ and } i,j = 1,\ldots,3 \\ 0 & i \neq j \end{cases} \tag{3}$$

If isotropic swelling is assumed, Eq. (3) becomes:

$$\varepsilon^{\text{s}}_{ij} = \frac{S(T)}{3}\delta_{ij} \tag{4}$$

with $\delta_{ij} = \begin{cases} 1 & \text{if } i=j \text{ and } i,j = 1,\ldots,3 \\ 0 & \text{if } i \neq j \end{cases}$ and where S denotes the swelling strain magnitude. In this work S can increase from 0 to a maximum prescribed value, $S_{\max}$, that is in general a function of the irradiation temperature and swelling regime. S represents the volumetric strain caused by irradiation-induced swelling.

The damage evolution law was obtained using the concepts of thermodynamics of continuous media [5–7] and a damage criterion dependent on a damage threshold function $F_c(T,D)$ [8,9]:

$$\mathrm{d}D = \frac{\frac{\partial C_{ijkl}(T,D)}{\partial D}\varepsilon^{\text{m}}_{ij}\mathrm{d}\varepsilon^{\text{m}}_{kl}}{\frac{\partial F_c(T,D)}{\partial D}} \tag{5}$$

Both tensile and shear strains contribute to increase damage, however damage is assumed not to be activated under a compressive state of stress. Damage evolution is computed incrementally per Eq. (5) until attaining the saturation state at which $D = D_{\text{cr}}$, and the material fails and can no longer carry load. Fracture is predicted to occur if $D = D_{\text{cr}}$ and is captured by a vanishing element technique [10,11]. In this work, a failure indicator is defined by the ratio D/D_{cr} to quantify how close the material is to fracture.

3. A dual-phase microstructural approach

3.1. Modeling domain

Fig. 1 presents a schematic of the dual-phase microstructural approach developed here to predict the microcracking mechanisms

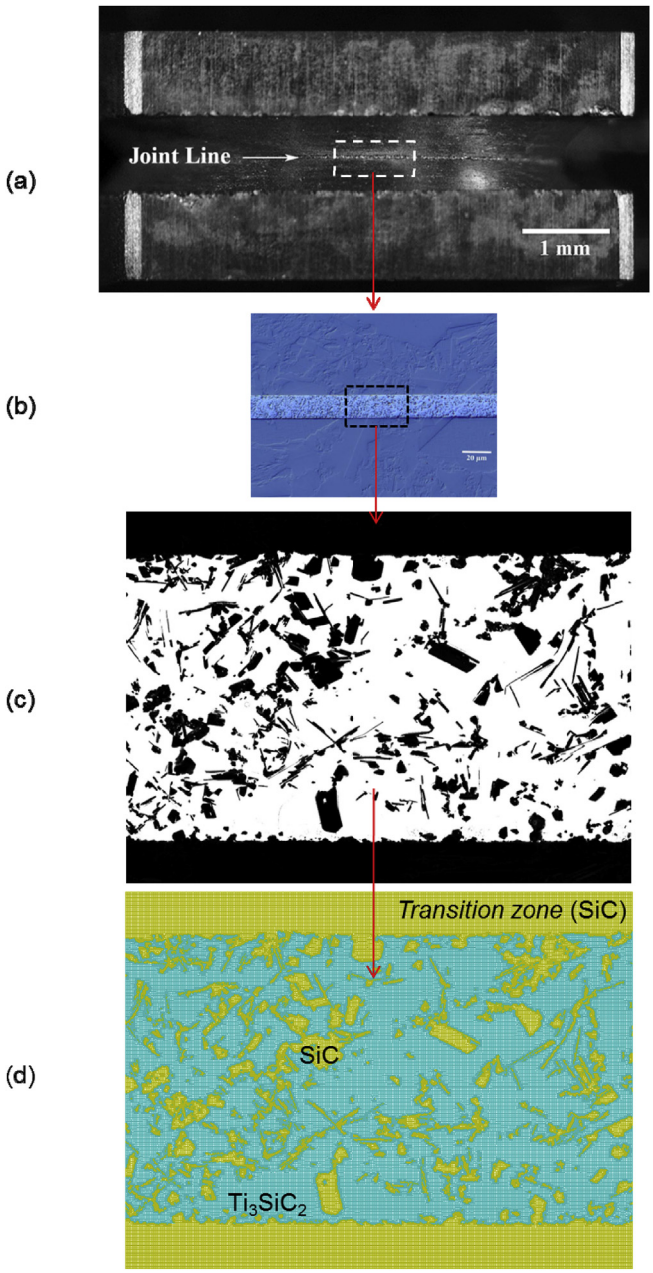

Fig. 1. Schematic of the dual-phase microstructural approach: (a) An as-formed THG specimen, (b) A micrograph taken from this specimen, (c) the digital image of the Ti_3SiC_2/SiC joint microstructure obtained from this micrograph, and (d) the finite element mesh built from the digital image using the OOF2 software.

occurring at the microstructural scale and are responsible for the Ti_3SiC_2/SiC joint damage observed in the experiments. Starting from an as-formed THG specimen illustrated in Fig. 1(a), a micrograph of the joint area including the SiC transition zone was taken as shown in Fig. 1(b). Next, a digital image of the Ti_3SiC_2/SiC microstructure including the SiC transition zones was created (Fig. 1(c)) to build the two-dimensional (2D) finite element (FE) mesh of this microstructure (Fig. 1(d)) using the OOF2[1] public domain software. Fig. 1(d) shows a very fine 2D FE mesh containing 251,055 elements over a 23 μm × 17 μm domain. Particularly, very

[1] Software developed at the National Institute of Standards and Technology.

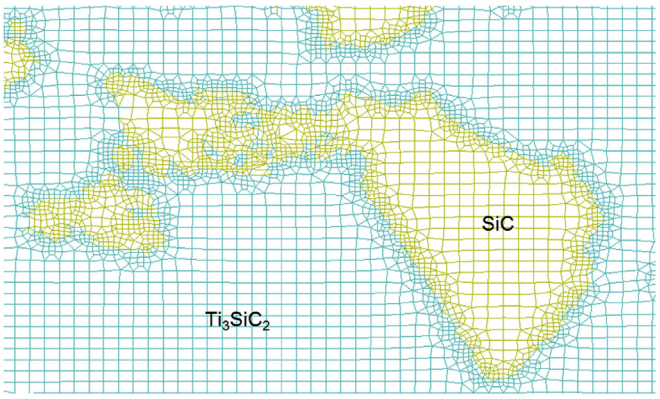

Fig. 2. A local snapshot showing the high-resolution mesh along the Ti_3SiC_2 and SiC boundaries.

fine discretizations were achieved along the boundaries between the Ti_3SiC_2 and SiC phases as illustrated in Fig. 2 that shows the detailed mesh in a local snapshot. The model uses continuum elements to discretize the individual phases, but it does not explicitly discretize the interfaces between different phases using e.g., cohesive finite elements. However, by very finely discretizing the interface regions, local stress concentrations along all the boundaries can be captured more accurately for damage and fracture analyses. If microcracking damage and fracture are predicted to develop in the elements along the interfaces ($D = D_{cr}$), then debonding between the individual phases sharing those interfaces occurs. Due to the lack of knowledge about the interface properties for a complete description of the interface debonding, the approach using cohesive finite elements would introduce more uncertainties into the model than the dual-phase continuum approach.

As the microstructural model is two-dimensional, it can only capture the microstructure morphology (e.g., phase shapes, phase distributions, etc.) in a simplified 2D manner, thus it cannot capture the features of the full 3D Ti_3SiC_2/SiC microstructure that varies from one location to another in the joint. Therefore, the local stresses, strains and damage evolution computed based on a 2D model can under- or over-predict the values computed based on a 3D model. However, as the FE model uses the constitutive laws presented in Section 2, it does capture the physics of the microcracking damage and fracture caused by the differential thermal expansion and irradiation-induced swelling.

3.2. Thermomechanical properties

The integration of the constitutive relation involving damage requires identification of the thermomechanical properties including the damage threshold function as a function of temperature for the temperature range of interest. This paper uses the same thermoelastic properties, i.e., elastic moduli and coefficients of thermal expansion (CTE), for SiC and Ti_3SiC_2 as collected in our recent paper [2] based on References [12–15]. Fig. 3(a) and (b) gather the temperature-dependent elastic modulus and CTE for SiC and Ti_3SiC_2 in the [25 °C, 800 °C] temperature range. For SiC, the functional representation by Snead et al. [12] for CVD SiC is used to obtain the elastic modulus of SiC as a function of temperature: $E = E_0 - BT\exp(T/T_0)$ where $E_0 = 460$ GPa, $B = 0.04$ GPa/K and $T_0 = 962$ K. The evolution of E with temperature expressed in degrees centigrade is given in Fig. 3(a), which also presents the data from Barsoum et al. [13] for Ti_3SiC_2. Fig. 3(b) presents the CTE evolution with temperature based on Barsoum et al. [14] and Gao et al. [15] for Ti_3SiC_2 as well as data from Ref. [12] for SiC.

While the same thermoelastic properties can be used for the same materials at different modeling scales from the micron scale of individual phases to the macroscale of a specimen, the strength of ceramics, thus the stress-strain response up to failure, is size-dependent. The size of a ceramic sample governs its strength, and this feature has been discussed in Refs. [12,16]. The report on characteristic strength of SiC based on different sources assembled in Ref. [12] clearly shows that the strength of SiC particles is substantially higher than the values for bulk SiC. According to [12], such a large variation is due to the specimen size effect related to the Weibull nature of failure. The size effect on fracture strength has also been discussed in Ref. [16] in terms of probability of fracture. Accordingly, the larger the size the smaller the fracture resistance since the probability that a severe flaw is present increases with size. These findings would suggest that damage model parameters identified for the bulk ceramic cannot be used for the ceramic phase at the particle or micron scale. The identification of the damage threshold function involved in Eq. (5) requires stress-strain data as functions of temperature. Therefore, it is necessary to determine the stress-strain responses of the micron-scale SiC and Ti_3SiC_2.

SEM experiments performed on unirradiated THG samples with the Ti_3SiC_2/SiC joint revealed that the bonding layer was intact before neutron irradiation at 800 °C. Therefore, in order to determine the magnitude of stresses that could be attained in the dual-phase domain subjected to heating up to 800 °C, which is the maximum temperature of interest in this study, the dual-phase Ti_3SiC_2/SiC model shown in Fig. 1(d) is allowed to deform *thermoelastically* due to heating from room temperature to 800 °C. Fig. 4 reports the stress solution obtained by the thermoelastic analysis of the dual-phase domain heated to 800 °C. Fig. 4(a) gives the phase distribution in the domain, and Fig. 4(b) and (c) respectively show the distributions of stress components, σ_{xx} and σ_{yy} in the modeling domain. Both σ_{xx} and σ_{yy} have attained very high values approaching 2200 MPa in the SiC phase while they are globally negative in Ti_3SiC_2 regions. With lower elastic modulus but much higher CTE (Fig. 3), the Ti_3SiC_2 phase can expand much more than the SiC phase resulting in tensile stresses in the SiC phase but compressive stresses in the Ti_3SiC_2 phase. The larger the mismatch of thermoelastic properties, the higher are the resulting stresses. As the joint was found to be intact at 800 °C before irradiation [1], it means that the strength of SiC at this temperature should be at the same order of magnitude as the values predicted by the thermoelastic solution. This is also consistent with the strength values reported for CVD SiC particles subject to hemisphere bend tests [12,17]. While fracture of the bulk ceramic is controlled by preexisting flaws or microvoids that form microcracks, the micron-scale ceramic that contains no flaws or a few flaws should have much higher strength and higher elongation at fracture (failure strain) than a bulk ceramic. In the absence of flaws, fracture of the micron-scale ceramic is controlled by the rupture of molecular bonds, and from a continuum damage modeling standpoint, this is reflected by very small values of the damage variable at fracture, D_{cr}.

In this work, using the elastic modulus from Fig. 3(a) and assuming $D_{cr} = 0.05$, and 0.5% failure strain for SiC in the [25 °C, 800 °C] temperature range, the tensile stress-strain response of SiC is established and illustrated in Fig. 5(a) for selected temperatures in this range. The resulting strength values at 0.5% failure strain are about 2200 MPa that match the strength data for particle SiC. Similar arguments are used to justify the stress-strain response of the micron-scale Ti_3SiC_2. In addition, we were also guided by the findings in Ref. [3] that the bending strength and toughness of a hot-pressed Ti_3SiC_2/SiC composite increased with temperature in the [25 °C, 800 °C] range. As the behavior of SiC is stable in the considered temperature range [12], the increase of this composite

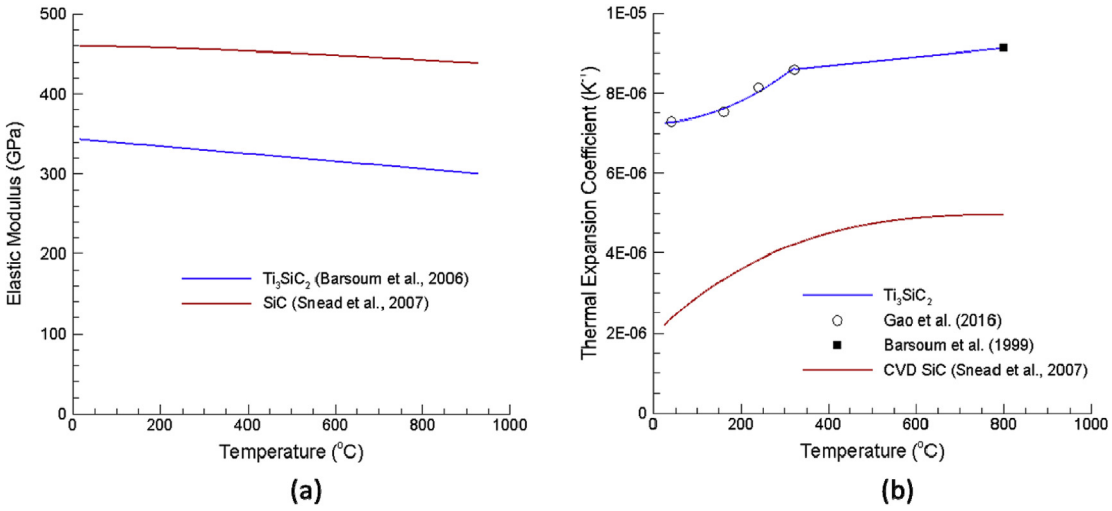

Fig. 3. Temperature-dependent elastic modulus (a) and CTE (b) for Ti_3SiC_2 [13–15] and SiC [12].

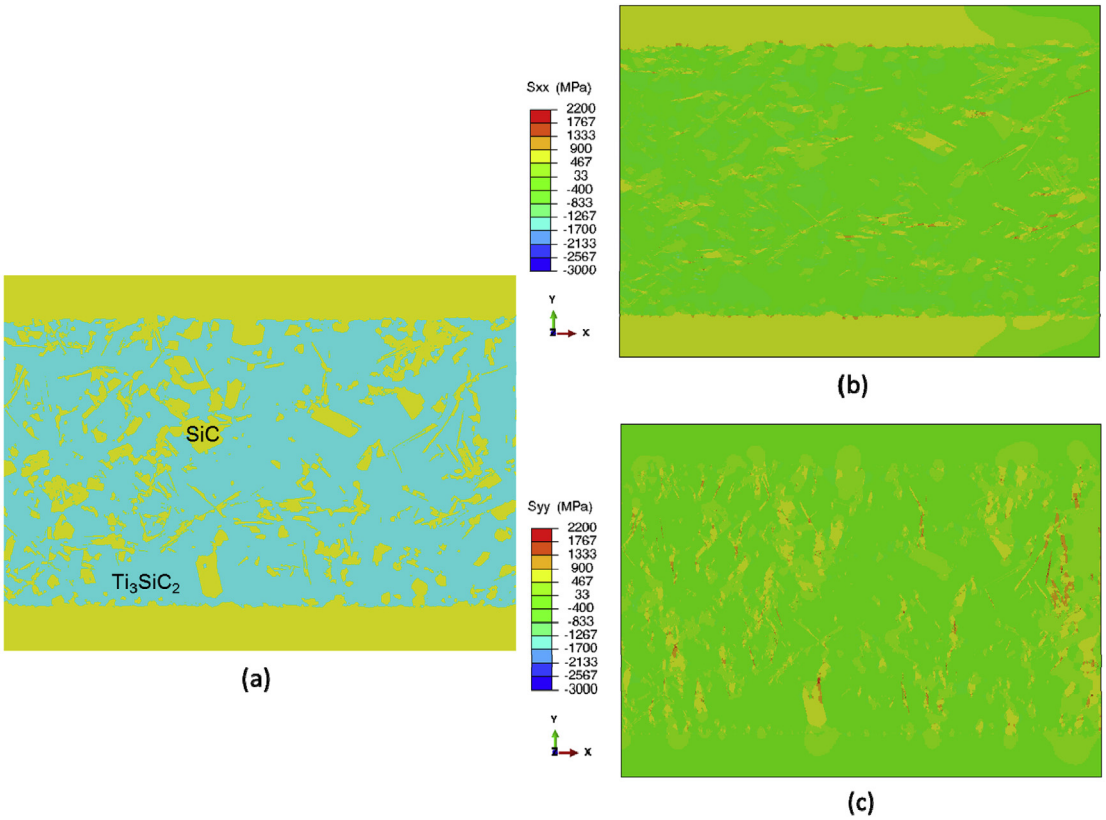

Fig. 4. (a) The Ti_3SiC_2/SiC joint microstructure, (b) Thermoelastic solutions for (b) σ_{xx}, and (c) σ_{yy} resulting from heating to 800 °C.

strength with temperature would be due to the temperature-dependent behavior of Ti_3SiC_2. These arguments were used to determine the tensile stress-strain response of the micron-scale Ti_3SiC_2 as a function of temperature in this paper. As for SiC, we consider the temperature-dependent elastic modulus of Ti_3SiC_2 given in Fig. 3(a) and the linear stiffness reduction relation with the damage variable. The stress-strain response of Ti_3SiC_2 is then computed as a function of temperature in the [25 °C, 800 °C] range assuming failure strains varying from 0.5% to 0.8% with D_{cr} from 0.05 to 0.1. The results for stress-strain response for the micron-scale Ti_3SiC_2 at selected temperatures are illustrated in Fig. 5(b). Using the method described in Ref. [9], the damage threshold functions for SiC and Ti_3SiC_2 are computed from the stress-strain responses in the [25 °C, 800 °C] range and illustrated in Fig. 6(a) and (b) for four selected temperatures in this range.

4. Results and discussion

The CDM model (Section 2) incorporating thermal expansion combined with irradiation-induced swelling effects was

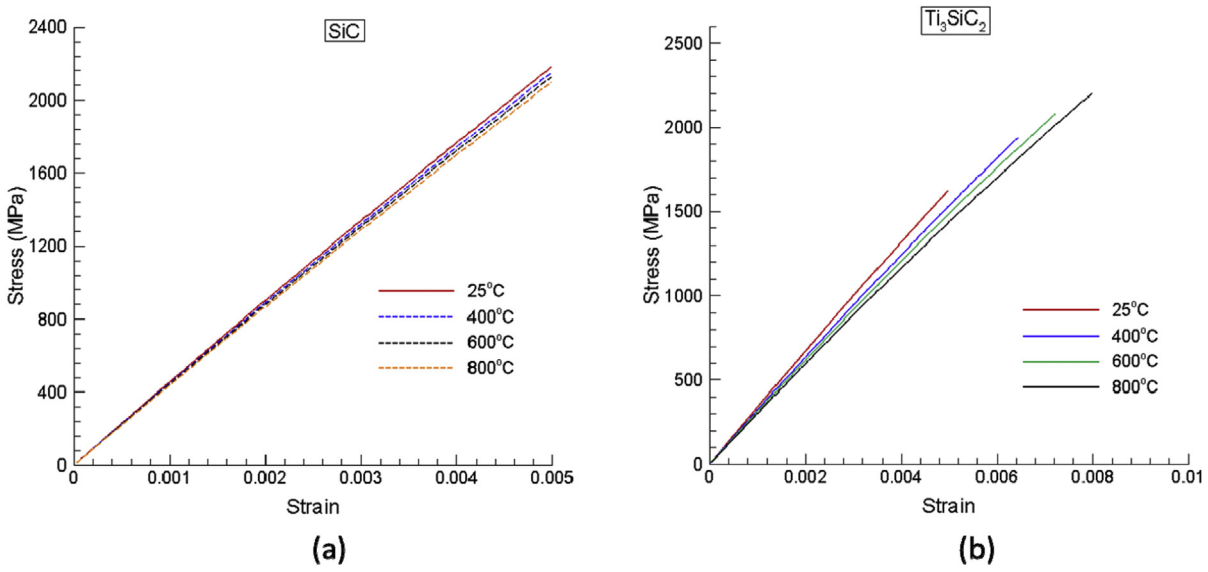

Fig. 5. Assumed temperature-dependent uniaxial tensile stress-strain responses for micron-scale (a) SiC and (b) Ti_3SiC_2.

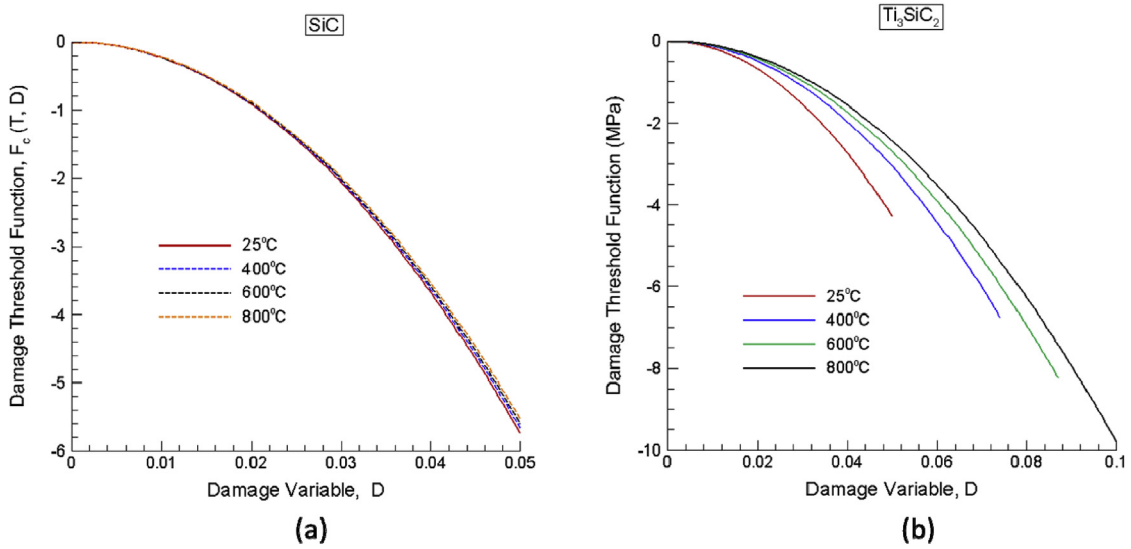

Fig. 6. The damage threshold functions for (a) SiC and (b) Ti_3SiC_2 calculated from the corresponding stress-strain responses assumed in Fig. 5.

implemented in the ABAQUS FE package by means of user-subroutines. In a recent paper [2], we have applied this model in ABAQUS's analyses of the THG joint specimen subjected to heating followed by irradiation-induced swelling at four prescribed irradiation temperatures (i.e., 800 °C, 500 °C, 400 °C> and 300 °C), and cooling to room temperature after irradiation swelling. In the present paper, the same damage model was used with ABAQUS to analyze the dual-phase Ti_3SiC_2/SiC microstructure subjected to heating to 800 °C followed by irradiation-induced swelling at this temperature, and cooling to room temperature. The 800 °C case was analyzed and is discussed in this paper to elucidate the joint damage mechanisms and their chronology considering the experimental observation of joint damage after neutron irradiation at 800 °C reported for this case [1]. At the micron scale, each phase region is a homogenous continuum, but the dual-phase domain is *heterogeneous*. This way damage can occur in the individual Ti_3SiC_2 and SiC phases and along their very finely discretized interfaces. The dual-phase domain (Fig. 1(d)) was not constrained to deform by external boundary conditions but can deform under the combined actions of thermal expansion and irradiation-induced swelling. It is important to emphasize that the dual-phase model is a typical representation of the materials and bonding joint at the *microstructural* level. The model is built through a digital image of the joint microstructure at a given location. As local phase distributions in shapes and volume fractions statistically vary from location to location, local distributions of stresses and strains as well as the extent of damage vary accordingly. However, the microcracking mechanisms identified should be similar or the same so that such a microstructural model can provide a deeper understanding of the origin of these mechanisms and their occurrence chronology in the bonded joint.

Fig. 7 shows the damage distribution in the dual-phase domain at the end of heating to 800 °C. Damage has been found to mainly develop in the SiC phase regions under local tensile/shear stress states. A few *transgranular* microcracks have been observed in some SiC phase regions corresponding to $D = D_{cr}$ as illustrated in more

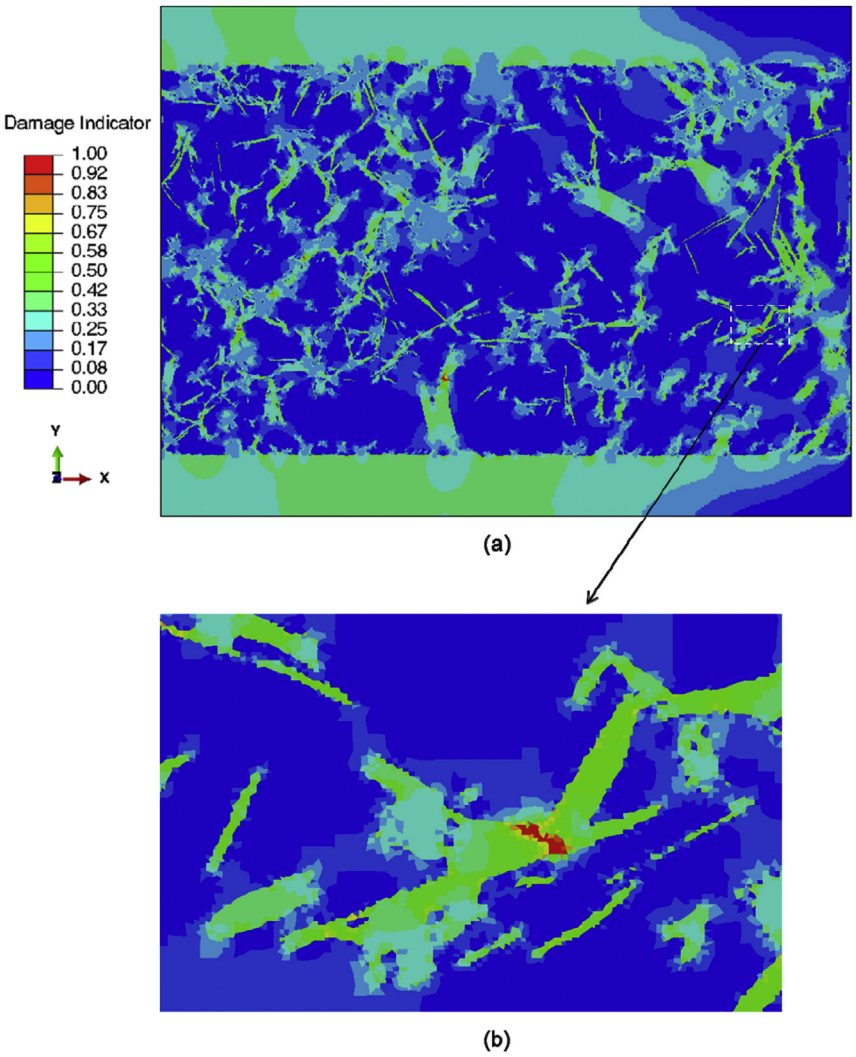

Fig. 7. Predicted damage distribution in: (a) the dual-phase domain at the end of heating to 800 °C, and (b) a local zoom-in showing a microcrack developed in SiC.

detail in Fig. 7(b) that shows a zoom-in of a local damage distribution involving a microcrack in SiC. The Ti_3SiC_2 regions undergoing compressive stresses appear to be practically intact after heating to 800 °C as indicated on Fig. 7(a) that shows zero or very small values of the damage indicator. The non-zero but very small values of the damage indicator have been observed mainly in the Ti_3SiC_2 regions along the boundaries between SiC and Ti_3SiC_2. Shearing along the boundaries between the tensile SiC and compressive Ti_3SiC_2 resulting from mismatches of thermoelastic properties has caused some damage in these interface regions, but damage is predicted to be negligible and no debonding has been found.

Once the dual-phase microstructure was brought to 800 °C, it was then subjected to irradiation-induced swelling at this temperature up to the respective maximum levels (0.8% for SiC [12] and 1.47% for Ti_3SiC_2 [18]). Fig. 8 shows the distribution of swelling in the dual-phase domain at the maximum prescribed swelling values. Important damage development has been found during swelling due to more pronounced concentrations of tensile stresses in SiC because the much higher swelling Ti_3SiC_2 is constrained in its expansion by the lower swelling SiC. Thus, the irradiation-induced swelling effect has added to the preceding thermal expansion effect causing significantly more damage to the dual-phase domain. Referring to Fig. 2(d), Fig. 9 clearly shows four types of microcracking mechanisms: (i) *transgranular microcracking* in SiC, (ii) *intergranular microcracking* along the SiC and Ti_3SiC_2 boundaries, (iii) *debonding* along the interfaces between the bonding joint and the SiC transition zones, and (iv) *transverse microcracking* of the SiC transition zone. Increased tensile stresses in SiC during irradiation-induced swelling have caused transgranular microcracking in SiC as this mechanism was already predicted after heating to 800 °C to a much lesser extent. High tensile stresses in the upper SiC transition zone also caused the transverse microcracking of this zone. Intergranular microcracking along SiC and Ti_3SiC_2 boundaries has been caused by important shear stresses that were further developed during swelling. The shear stresses were also responsible for the debonding predicted along the interfaces between the bonding joint and the SiC transition zones.

After irradiation swelling, the dual-phase domain model was uniformly cooled to room temperature. The damage and fracture development at the end of cooling presented in Fig. 10 clearly shows the same types of microcracking mechanisms predicted at the end of irradiation swelling. The mismatch of the thermal contractions (due to the mismatch of thermomechanical properties) between SiC and Ti_3SiC_2 combined with the mismatch of

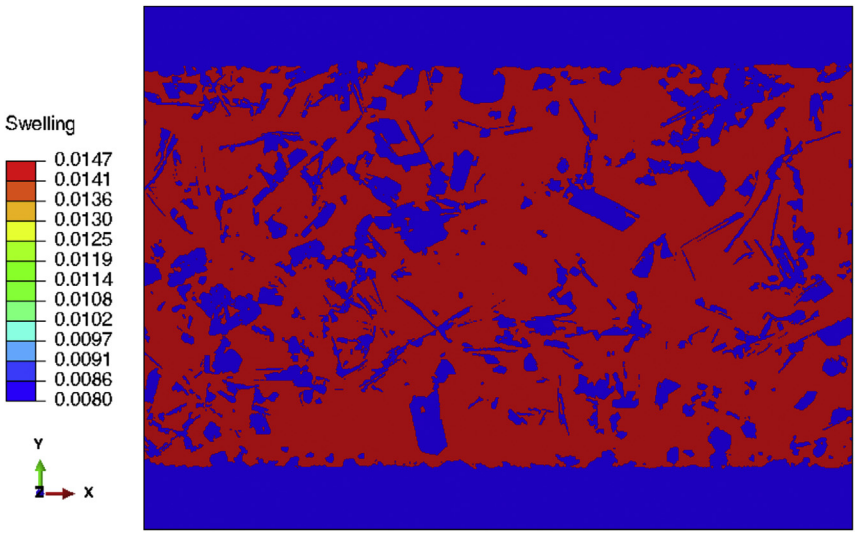

Fig. 8. Simulated irradiation-induced swelling at 800 °C.

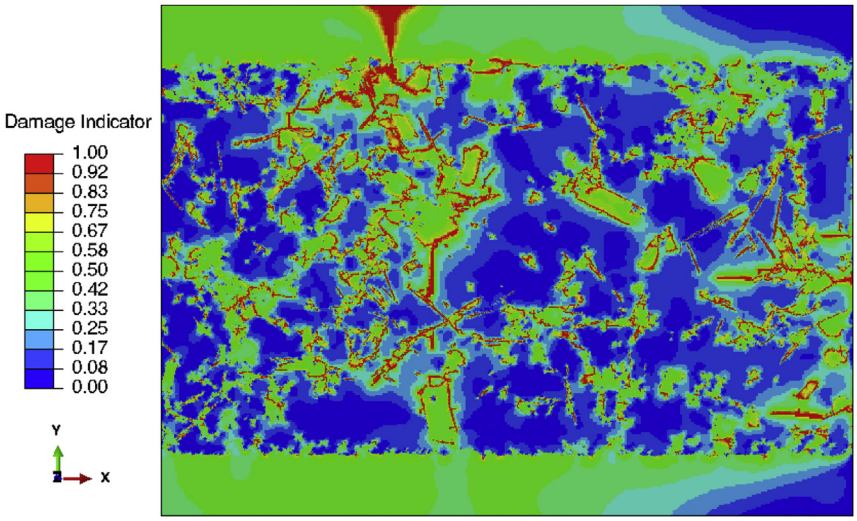

Fig. 9. Predicted damage and fracture developments in the dual-phase domain after irradiation-induced swelling at 800 °C.

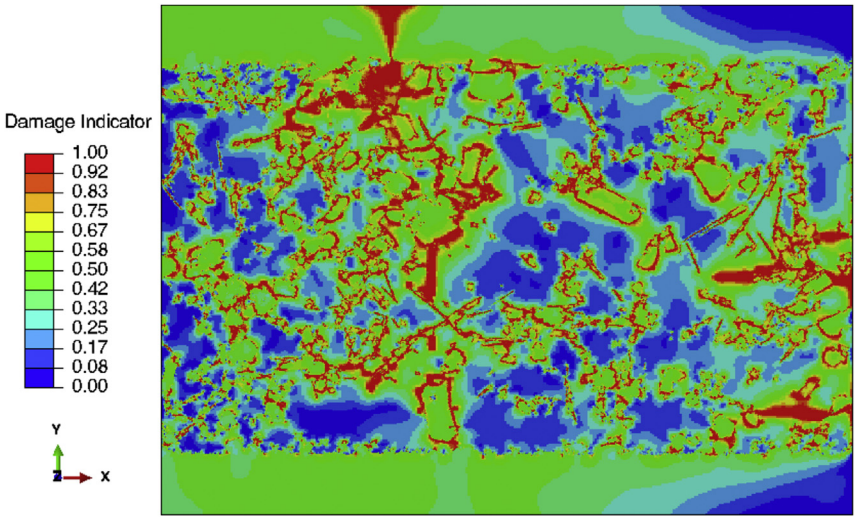

Fig. 10. Predicted damage and fracture developments in the dual-phase domain after cooling to room temperature.

irreversible swelling strains increased the shear strains along the fractured SiC and Ti_3SiC_2 boundaries leading to further damage and fracture of these boundaries during cooling to room temperature. That also caused increase in local tensile stresses that triggered the propagation of existing cracks (initiated during irradiation induced swelling). Comparing Fig. 9 to Fig. 10 clearly shows intensified crack development along the SiC and Ti_3SiC_2 boundaries and amplification of existing cracks after cooling to room temperature. The prediction of these mechanisms due to combined thermal and irradiation-induced swelling effects appears to globally agree with the experimental observation about the presence of microcracks in the joint after the irradiation experiment of the THG specimen at 800 °C [1].

5. Conclusions

A dual-phase microstructural approach is developed to simulate the progressive microcracking mechanisms observed in the Ti_3SiC_2/SiC joint of THG specimens subjected to heating to 800 °C followed by neutron irradiation at this temperature, and cooling to room temperature after irradiation. The approach uses an actual microstructural domain involving individual SiC and Ti_3SiC_2 phases finely discretized and whose behaviors are described by the continuum damage mechanics model reported in our recent article [2]. We have explored observed size effects on ceramic material strength to establish the stress-strain responses of micron-scale SiC and Ti_3SiC_2 allowing the application of this damage model at the microstructural scale. We have applied the damage model implemented in ABAQUS to analyze the dual-phase Ti_3SiC_2/SiC microstructural domain subjected to similar experimental conditions as the THG specimen with the Ti_3SiC_2/SiC bonding joint experienced during neutron irradiation testing. The following conclusions can be drawn for the analysis results:

- Four distinct microcracking mechanisms are predicted: (i) *transgranular microcracking* in SiC, (ii) *intergranular microcracking* along the grain boundaries of Ti_3SiC_2 and SiC, (iii) *debonding* between the bonding joint and the SiC transition zones, and (iv) *transverse microcracking* of the SiC transition zone.
- *Heating to 800°C*: We have generally found minor damage with a few transgranular cracks in SiC.
- *Irradiation-induced swelling at 800°C*: Significant damage and fracture developments are predicted involving all the identified mechanisms.
- *Cooling to room temperature*: Further damage and fracture developments due to these mechanisms are found in the cracked domain suffering from irreversible swelling strains combined with thermal contraction

The dual-phase microstructural approach developed in this paper depends on the local microstructure that varies statistically from location to location in terms of domain size and strength. Since strengths of ceramics at the micron scale also vary significantly and are not very well known, damage and fracture predictions based on a single typical microstructure with the assumed mechanical behaviors for the constituent phases could over-predict or under-predict the actual damage and fracture states observed after irradiation experiments. Also, the modeling performed at the microstructural scale alone can help describe the deformation and damage mechanisms but cannot produce the actual constraints that macroscopic specimens experience. In addition, the model developed here does not include any time-dependent material properties, such as irradiation creep or thermal creep that would likely modify these results. These mechanisms were not included since that data does not yet exist for the Ti_3SiC_2 phase. Future models will include these mechanisms.

Amid these uncertainties, the dual-phase microstructural approach appears to reasonably capture the microcracking mechanisms and their occurrence chronology observed in limited experiments. This approach has been demonstrated to be effective and robust, and can be readily extended to involve more phases that exist in an actual microstructure of a ceramic composite joint. Although our current 2D FE model can be extended to 3D FE models, it can be used to optimize composite microstructure through phase distributions, operating conditions or limits in terms of temperature range and dose to minimize damage to support neutron irradiation-based design of joined ceramics and composites in conjunction with structural analyses of components and in-reactor testing.

Acknowledgements

This research was supported by U.S. Department of Energy, Office of Fusion Energy Sciences under Contract DE-AC05-76RL01830. PNNL is a multi-program national laboratory operated by Battelle Memorial Institute for the US DOE under DE-AC06-76RLO 1830.

References

[1] Y. Katoh, L.L. Snead, T. Cheng, C. Shih, W.D. Lewis, T. Koyanagi, T. Hinoki, C.H. Henager Jr., M. Ferraris, J. Nucl. Mater. 448 (1–3) (2014) 497–511.
[2] B.N. Nguyen, C.H. Henager Jr., R.J. Kurtz, Modeling thermal and irradiation-induced swelling effects on the integrity of Ti3SiC2/SiC joints, J. Nucl. Mater. 495 (2017) 504–515.
[3] Henager Jr., R.J. Kurtz, J. Nucl. Mater. 417 (2011) 375–378.
[4] M. Ben-Belgacem, V. Richet, K.A. Terrani, Y. Katoh, L.L. Snead, J. Nucl. Mater. 447 (2014) 125–142.
[5] J. Lemaître, J.-L. Chaboche, Mécanique des Matériaux Solides, Dunod, Paris, France, 1985.
[6] G.A. Maugin, The Thermomechanics of Plasticity and Fracture, Cambridge University Press, Cambridge, UK, 1992.
[7] J. Lemaitre, in: O. Allix, F. Hild (Eds.), Continuum Damage Mechanics of Materials and Structures, Elsevier Science Ltd, Oxford, UK, 2002, pp. 235–258.
[8] J. Renard, J.P. Favre, T. Jeggy, Compos. Sci. Technol. 46 (1) (1993) 29–37.
[9] B.N. Nguyen, B.J. Koeppel, S. Ahzi, M.A. Khaleel, P. Singh, J. Am. Ceram. Soc. 89 (4) (2006) 1358–1368.
[10] V. Tvergaard, Int. J. Fract. 31 (3) (1986) 183–209.
[11] B.N. Nguyen, V. Kunc, Int. J. Damage Mech. 19 (6) (2010) 691–725.
[12] L.L. Snead, T. Nozawa, Y. Katoh, T.-S. Byun, S. Kondo, D.A. Petti, J. Nucl. Mater. 371 (1–3) (2007) 329–377.
[13] M.W. Barsoum, M. Radovic, A. Ganguly, T. Zhen, P. Finkel, S.R. Kalidindi, E. Lara-Curzio, Acta Mater. 54 (10) (2006) 2757–2767.
[14] M.W. Barsoum, T. El-Raghy, C.J. Rawn, W.D. Porter, H. Wang, E.A. Payzant, C.R. Hubbard, J. Phys. Chem. Solids 60 (4) (1999) 429–439.
[15] H. Gao, R. Benitez, W. Son, R. Arroyave, M. Radovic, Mater. Sci. Eng. A 676 (2016) 197–208.
[16] J. Lamon, in: Brittle Fracture and Damage of Brittle Materials and Composites, ISTE Press Ltd. Published by Elsevier Ltd, Oxford, UK, 2016, pp. 109–132.
[17] A. Briggs, R.W. Davidge, C. Padgett, S. Quickenden, J. Nucl. Mater. 61 (1976) 233–242.
[18] C. Ang, S. Zinkle, C. Shih, C. Silva, N. Cetiner, Y. Katoh, J. Nucl. Mater. 483 (2017) 44–53.